The $C_4H_8^{\bullet+}$ Potential Energy Surface. 1. The Cyclobutane Radical Cation

Pavel Jungwirth,† Petr Čársky,† and Thomas Bally*,‡

Contribution from the Institut de Chimie Physique, Université de Fribourg, Perolles, 1700 Fribourg, Switzerland, and J. Heyrovský Institute of Physical Chemistry and Electrochemistry, Academy of Sciences of the Czech Republic, Dolejskova 3, 182 23 Prague 8, Czech Republic

Received September 22, 1992

Abstract: The potential energy surface of the cyclobutane radical cation ($CB^{\bullet+}$) has been explored at the QCISD-(T)/6-31G*//UMP2/6-31G* level of theory. Thereby it was found that the first-order Jahn–Teller rhombic and rectangular structures are more stable than the long-bond trapezium structure reported to be the global minimum on the $CB^{\bullet+}$ surface in previous semiempirical and ab initio SCF calculations. In agreement with ESR experiments, a rhombic structure very flexible to ring puckering was found to be the most stable one. Methyl-, *trans*-1,2-dimethyl-, *trans*-1,3-dimethyl-, and *all-trans*-tetramethyl-$CB^{\bullet+}$ were calculated at the UMP2/6-31G*//UHF/6-31G* level. These studies revealed that the long-bond trapezoidal structure is favored by the influence of electron-releasing substituents to the extent that it represents the global minimum for *trans*-1,2-dimethyl-$CB^{\bullet+}$.

I. Introduction

Cyclobutane (CB) is one of the cardinal organic hydrocarbons, and the CB moiety forms part of a great number of structures of relevance to aspects of natural product as well as technical chemistry. In particular, CB and related organic molecules were found to be involved in charge-transfer processes of different types in the gas as well as in the condensed phase.[1] It would therefore appear that a correct understanding of the properties of the cyclobutane radical cation ($CB^{\bullet+}$) should form the basis for explanations of the multifaceted phenomena encountered in such contexts. However, as of now, theory and experiment have yielded conflicting evidence regarding the molecular and electronic structure of $CB^{\bullet+}$. For example, ESR experiments have been interpreted in terms of a puckered rhomboidal structure[2] while most calculations predict a planar trapezoidal equilibrium geometry.[3-7]

Removal of an electron from the degenerate HOMO of cyclobutane in its (puckered) square equilibrium geometry of D_{2d} symmetry leads to the ^2E_u ground state of $CB^{\bullet+}$. If we assume for the sake of argument that $CB^{\bullet+}$ is planar (the possibility of puckering will be examined and discussed below), it can undergo first-order Jahn–Teller (FOJT) distortions[8a] along a b_{1g} normal mode leading to a rhombus and along a b_{2g} mode leading to a rectangle, both of D_{2h} symmetry (see Figure 1).

In previous calculations on $CB^{\bullet+}$, two additional geometries of C_{2v} symmetry were considered which were thought to arise as a consequence of second-order Jahn–Teller (SOJT) distortions.[8b] These distortions which deform the rectangle (or the square) to a trapezium and the rhombus (or the square) to a kite (Figure 1) may arise through mixing of the ground state with one or several low-lying excited configurations upon descent to C_{2v} symmetry.

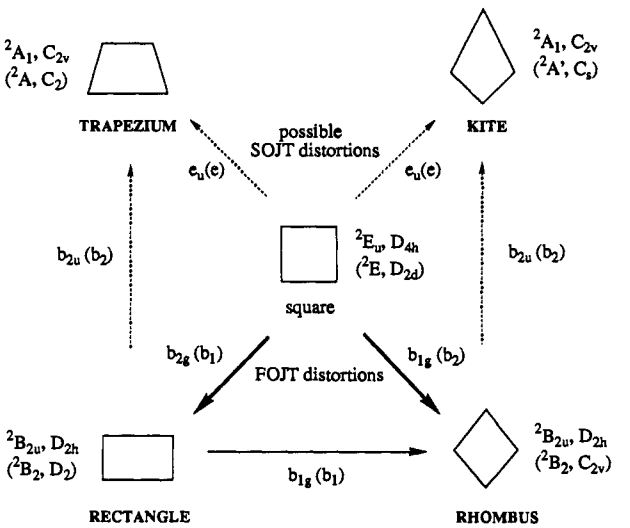

Figure 1. Jahn-Teller distortions of square cyclobutane radical cation (data in parentheses correspond to puckered geometries).

Most experimental studies on $CB^{\bullet+}$ prior to 1982 were concerned with the energetics and dynamics of the ionization process as well as possible rearrangement pathways in the gas phase.[1] Although the possible Jahn–Teller (JT) distortions of $CB^{\bullet+}$ received occasional attention, this aspect was not subjected to any systematic scrutiny until after Iwasaki et al.[2] proposed on the basis of ESR evidence that $CB^{\bullet+}$ exists in the form of a $^2B_2$ state of puckered rhomboidal geometry at 4 K in $CFCl_3$. This finding spurred three theoretical investigations whose results will be briefly reviewed.

The first of these studies[9] came from the group of Shida, which had also participated in the pivotal experimental work cited above. It reported on ab initio UHF/STO-4G calculations which explored

† Academy of Sciences of the Czech Republic.
‡ University of Fribourg.
* To whom correspondence should be addressed.

(1) See e.g. van Velzen, P. N. T.; van der Hart, W. *J. Chem. Phys.* **1981**, *61*, 335. Hsier, T.; Gilman, J. P.; Weiss, M. J.; Meisels, G. G. *J. Phys. Chem.* **1981**, *85*, 2722. Greathead, R. J.; Jennings, K. R. *Org. Mass Spectrom.* **1980**, *15*, 431 and references therein.

(2) Ushida, K.; Shida, T.; Iwasaki, M.; Toriyama, K.; Nunome, K. *J. Am. Chem. Soc.* **1983**, *105*, 5496.

(3) Lee, T.-S.; Lien, M. H.; Jen, S.-F.; Ou, M.-C.; Wu, H.-F.; Gau, Y.-F.; Chang, T.-Y. *J. Mol. Struct. THEOCHEM* **1988**, *170*, 121.

(4) Dewar, M. S.; Merz, K. M., Jr. *J. Mol. Struct. THEOCHEM* **1985**, *122*, 59.

(5) Pabon, R. A.; Bauld, N. L. *J. Am. Chem. Soc.* **1984**, *106*, 1145.

(6) Bauld, N. L.; Bellville, D. J.; Pabon, R.; Chelsky, R.; Green, G. *J. Am. Chem. Soc.* **1983**, *105*, 2378.

(7) Bellville, D. J.; Bauld, N. L. *J. Am. Chem. Soc.* **1982**, *104*, 5700.

(8) (a) Jahn, H. A.; Teller, E. *Proc. R. Soc. London, A* **1937**, *161*, 220. Bader, R. F. W. *Can. J. Chem.* **1962**, *40*, 1164. (b) Pearson, R. G. *J. Am. Chem. Soc.* **1969**, *91*, 4947.

(9) Ohta, K.; Nakatsuji, H.; Kubodera, H.; Shida, T. *Chem. Phys.* **1983**, *76*, 271.

0002-7863/93/1515-5776$04.00/0

the two possible modes of FOJT distortions of D_{2d} (puckered square) $CB^{\bullet+}$ along b_1 and b_2 normal coordinates leading to geometries of puckered rectangular (C_2) and rhomboidal (C_{2v}) shapes, respectively. They found the latter form to be slightly less stable than the former in an apparent contradiction with the ESR findings.[2] However, in contrast to later studies, they actually admitted ring puckering and indeed their FOJT structures turned out to be significantly nonplanar.

Shortly thereafter, Radom et al.[10] published the results of a more comprehensive investigation. In the introduction to their first paper,[10a] they give a general outline of the qualitative features of the $CB^{\bullet+}$ potential energy surface (P.E.S.), accounting for the first time also for the possibility of SOJT distortions. They performed UHF/3-21G geometry optimizations on the D_{2h} geometries (rectangle and rhombus) and C_{2v} structures (trapezium and kite) enforcing D_{2h} and C_{2v} symmetry, respectively. Upon relaxing the symmetry constraints, all their structures collapsed to a trapezium. They continued by MP2/3-21G single-point calculations and an estimation of the MP2/6-31G* energies. At the latter level, the order of C_{2v} and D_{2h} structures was reversed and the rhombus became the most stable one.

Both of the above ab initio studies which explored different aspects of the $CB^{\bullet+}$ P.E.S. suffered from the drawback that the nature of the points corresponding to the optimized geometries was not investigated. This problem received special attention in a later study by Dewar and Merz,[4] who applied the MNDO model using the RHF "half electron" procedure, which allowed them to properly characterize stationary points by diagonalizing the matrix of second derivatives. Thus they found only one true minimum corresponding to a planar trapezoidal structure which was surrounded by three other (planar) stationary points lying some 2–3 kcal/mol higher in energy: a parallelogram which serves as a transition state for the interconversion of two equivalent trapezia (the rectangle was found to be a hilltop 0.01 kcal/mol higher in energy than the parallelogram) and 0.5 kcal/mol above that a rhombic transition state interconnecting pairs of equivalent parallelograms. On the basis of these results, Dewar and Merz[4] called for a reinterpretation of the ESR spectra[2] of $CB^{\bullet+}$ in terms of rapidly interconverting trapezoidal rather than a static rhomboidal structure.

The P.E.S. of $CB^{\bullet+}$ has also been investigated from the point of view of the symmetry-forbidden ethylene–ethylene radical cation cycloaddition reaction.[3,5-7] This section of the $C_4H_8^{\bullet+}$ P.E.S. will be examined in part II of this study. It suffices to say at this point that the activation energy for formation of $CB^{\bullet+}$ from ethylene and ethylene radical cation is greatly reduced from the value for the neutral reaction although the reaction remains symmetry forbidden.

In the present paper we (re)investigate sections of the P.E.S. of $CB^{\bullet+}$ relevant to Jahn–Teller (JT) distortions. Some alkylated derivatives of $CB^{\bullet+}$ are studied to obtain an idea about the influence of substituents on the JT distortions. In order to shed new light on the somewhat confusing picture of the structure and energetics of $CB^{\bullet+}$ from recent literature, our calculations were performed on ab initio post-SCF levels including MBPT, CI, and MCSCF approaches using large basis sets.

In section II we outline the computational strategy applied in this work. After a brief discussion of neutral CB in section III, the JT surface of $CB^{\bullet+}$ is described in section IV, and the results of calculations on its alkylated derivatives are presented in section V. Finally, our findings are summarized and discussed in section VI.

II. Computational Methods

The goal of our work was to get, is possible, a 'definitive' picture of relevant sections of the P.E.S. of $CB^{\bullet+}$. Therefore, we had to begin by defining a level of theory for the full study at which a further improvement of the method of accounting for dynamic and nondynamic correlation effects and/or an augmentation of the basis set would be unlikely to change the picture in any fundamental way.

It had already become evident from the earlier study of Radom et al.[10a] that correlation plays a crucial role, but we found that this effect could be accounted for satisfactorily by many-body perturbation theory carried to the second order. Thus, optimizations were performed at the UMP2/6-31G* level under various symmetry constraints. On the condition that the UHF wave function is not strongly contaminated by higher spin components (which turned out to be the case throughout all sections of the P.E.S. of $CB^{\bullet+}$ which are relevant to the present study), the UMP2 method should give reliable results. Unless stated otherwise, the 6-31G* basis set was used throughout our study.

All stationary points were examined by a UMP2/6-31G* vibrational analysis which also provided values for zero-point vibrational energies (ZPE). Single-point energy calculations at the optimized geometries were performed both on the UMP2/6-311G** level and by a variant of the CC-SD(T) method (called QCISD(T) in *Gaussian*[11a]) using again the 6-31G* basis set. The purpose of these calculations was to check for saturation of basis set and correlation effects. In order to check for the possibility of significant nondynamic correlation effects, all important points on the P.E.S. were recalculated (and some reoptimized) using a CASSCF procedure with seven electrons in eight active orbitals (four bonding and four antibonding σ-MO's of the carbon frame), using the GAMESS program.[11b]

Since we found that, under appropriate symmetry restrictions on the carbon frame of $CB^{\bullet+}$, the UHF geometries differ very little from those optimized on the UMP2 level, the mono-, di-, and tetramethyl derivatives of $CB^{\bullet+}$ were optimized at the UHF level followed by single-point UMP2 energy evaluations. The complete set of MO's was included for correlation during UMP2 geometry optimizations, as this allows for the use of analytical gradients in *Gaussian90*.[11a] However, all post-SCF energies reported in this paper were eventually calculated with frozen carbon 1s orbitals.

In order to relate our findings to the experiments of Iwasaki et al.,[2] we evaluated ESR coupling constants for various geometries of $CB^{\bullet+}$ at different levels of theory ranging from ROHF/6-311G** to CISD/6-31G*. These calculations were performed using the MELD program package.[11c]

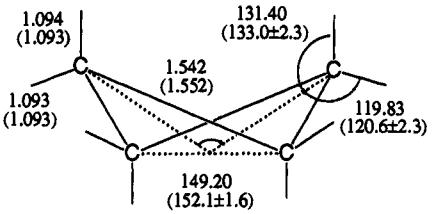

NEUTRAL CYCLOBUTANE (D_{2d})

Figure 2. MP2/6-31G* optimized structure of cyclobutane. Values in parentheses are from the recent electron diffraction study of Egawa et al.[13]

III. Neutral Cyclobutane

As a test of our computational methods with regard to a correct description of the geometry and the inversion barrier in the title system, we calculated the equilibrium structure of neutral CB at the MP2/6-31G* level.[12] The results are compared to the best

(10) (a) Bouma, W. J.; Poppinger, D.; Radom, L. *J. Mol. Struct. THEOCHEM* **1983**, *103*, 209. (b) *Isr. J. Chem.* **1983**, *23*, 21.

(11) (a) Frisch, M. J.; Head-Gordon, M.; Trucks, G. W.; Foresman, J. B.; Schlegel, H. B.; Raghavachari, K.; Robb, M. A.; Binkley, J. S.; Gonzales, C.; DeFrees, D. J.; Fox, D. J.; Whiteside, R. A.; Seeger, R.; Melius, C. F.; Baker, J.; Martin, R. L.; Kahn, L. R.; Steward, J. J. P.; Topiol, S.; Pople, J. A. *Gaussian 90*; Gaussian, Inc.: Pittsburgh, PA, 1990. (b) Schmidt, M. W.; Baldridge, K. K.; Boatz, J. A.; Jensen, J. H.; Koseki, S.; Gordon, M. S.; Nguyen, K. A.; Windus, T. L.; Elbert, S. T. GAMESS. *QCPE* **1990**, *10*, 52. (c) The MELD suite of programs was developed by Davidson, E. R., and co-workers, Department of Chemistry, Indiana University, Bloomington, IN.

(12) For results at the SCF level we refer to the earlier work of Cremer (Cremer, D. *J. Am. Chem. Soc.* **1977**, *99*, 1307).

Table I. RHF, MP2, and QCISD(T) Energies for Two Geometries of Neutral CB (Optimized at MP2/6-31G*) and UHF, UMP2, and QCISD(T) Energies for Five Geometries of $CB^{\bullet+}$ (Optimized at UMP2/6-31G* Except for the Kite and Trapezium)

	UHF(RHF)/ 6-31G*	(U)MP2/ 6-31G*	(U)MP2/ 6-311G**	QCISD(T)/ 6-31G*
CB puckered[a]	−156.096448	−156.61800	−156.73546	−156.68277
CB planar[b]	0.7	2.2		1.8
$CB^{\bullet+}$ rhombus[a]	−155.759331	−156.26915	−156.37701	−156.33318
$CB^{\bullet+}$ rectangle[c,d]	−3.7	1.9	1.5	1.1
$CB^{\bullet+}$ kite[c,e]	−2.1	5.8	5.6	3.1
$CB^{\bullet+}$ trapezium[c,e]	−9.4	7.8	8.0	3.5
$CB^{\bullet+}$ square[c,f,g]	29.9	27.7		27.4
$CB^{\bullet+}$ square[c,g]	22.1	20.8	21.3	21.4

[a] Total energy in au. [b] Energy relative to puckered CB in kcal/mol. [c] Energy relative to rhombus in kcal/mol. [d] Corrected by the ZPE difference (+0.32 kcal/mol) calculated at the UMP2/6-31G* level. [e] UHF/6-31G* optimized geometries. [f] At equilibrium geometry of neutral CB. [g] "Rectangular" MO's.

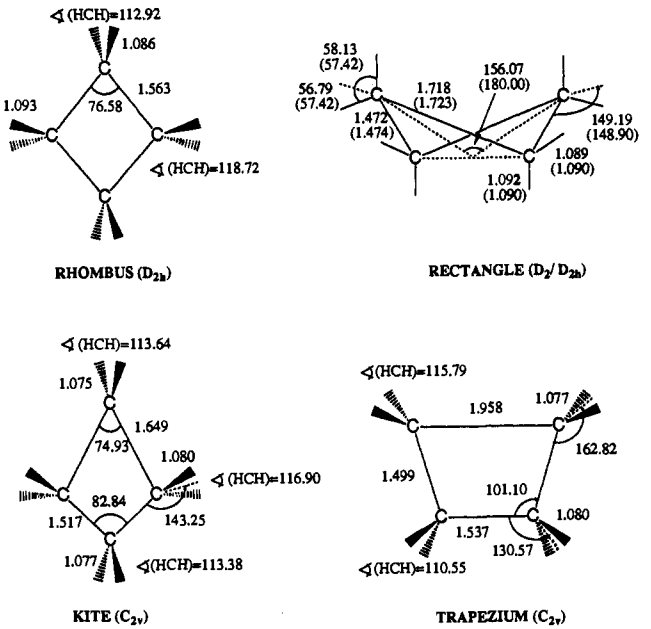

Figure 3. UMP2/6-31G* optimized geometries of the rhombus and the rectangle and UHF/6-31G* optimized geometries for trapezium and kite. For the rectangle the values in parentheses correspond to a planar geometry.

available experimental values[13] in Figure 2 while the energies are listed in the first two rows of Table I. Agreement with the recent electron diffraction data[13] is close to the experimental uncertainty for all structural parameters, but in spite of the fact that the puckering angle is slightly underestimated, the inversion barrier (experimental: 1.4 kcal/mol[13]) is overestimated by 60% at the MP2 and by 30% at the QCISD(T) level. However, the absolute errors (0.8 and 0.4 kcal/mol, respectively) are quite small, and thus we can expect that the MP2/6-31G* method is also well suited to model the puckering in $CB^{\bullet+}$.

IV. Jahn–Teller Surface of $CB^{\bullet+}$: Results

To establish a connection with previous theoretical studies[3-7] we first performed UHF optimizations of D_{2h} (rhombus and rectangle) and C_{2v} structures (trapezium and kite) and of the D_{4h} square geometry. At this level a trapezium was found to be the most stable structure, followed by a rectangle, a kite, and a rhombus. When the D_{2h} structures were reoptimized within C_{2v} symmetry, the rectangle collapsed to the trapezium and the rhombus to the kite (for optimized geometries see Figure 3).

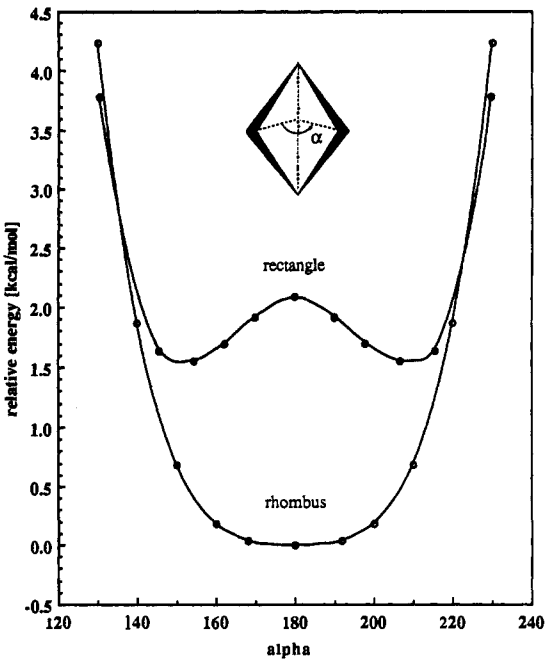

Figure 4. Relative UMP2/6-31G* energies of the rhombus and the rectangle as a function of the puckering angle α. (Geometries were reoptimized with UMP2/6-31G* at each step.)

Vibrational analysis at this level revealed that the trapezium is a minimum except for a small imaginary frequency of −83 cm^{-1}, corresponding to ring puckering. The other three structures were marginally stable with respect to puckering (the corresponding frequencies varying from +30 to +100 cm^{-1}), the rectangle being a saddle point between the two equivalent trapezia, the kite having one imaginary frequency corresponding also to a distortion toward the trapezium, and the rhombus having two negative frequencies associated with distortions toward kite and rectangular (via parallelogram) geometries. The UHF wave functions suffered very little from spin contamination ($\langle S^2 \rangle < 0.77$), and as additional calculation showed, the geometries as well as the relative energies of the four structures were nearly identical using either UHF or ROHF wave functions.

Single-point UMP2/6-31G* energy estimates at UHF/3-21G optimized geometries had already revealed earlier that the simple HF model is probably not appropriate for the case of $CB^{\bullet+}$, as the order of the energies of the D_{2h} and C_{2v} structures was reversed.[10] Therefore we reoptimized the structures at the UMP2 level within D_{2h} and C_{2v} symmetry, respectively. In contrast to the HF calculations, only two stationary points were found as the trapezium collapsed to the rectangle and the kite to the rhombus (cf. Figure 3). However, it should be recalled that the UHF and UMP2 optimized geometries for the D_{2h} structures are nearly identical and that the UHF as well as UMP2 energy difference between the two geometries is <1 kcal/mol for both the rhombus and the rectangle. This may serve as a justification for comparing energies calculated at UMP2 geometries (rhombus, rectangle, and square) with those of the UHF optimized structures (trapezium and kite) in Table I.

In a second step UMP2 optimizations were performed without any symmetry constraints, as a result of which all geometries collapsed to the rhombus. Vibrational analysis on the same level confirmed that the rhombus is a true minimum marginally stable toward puckering, the corresponding vibrational frequency being +37 cm^{-1}. For the (planar) rectangle we found two imaginary frequencies: one of −265 cm^{-1} associated with a distortion toward a rhombus via a parallelogram and second of −121 cm^{-1} corresponding to ring puckering. Reoptimization of the rectangle within D_2 symmetry (allowing for puckering) resulted in an energy gain of only 0.5 kcal/mol, which was, however, accompanied by

(13) Egawa, T.; Fukuyama, T.; Yamamoto, S.; Takabayashi, F.; Kambara, H.; Ueda, T.; Kuchitsu, K. *J. Chem. Phys.* **1987**, *86*, 6018.

Table II. UHF, CASSCF, and UMP2 Energies for UMP2 Optimized Rhombic[a] and Square[b] $CB^{\bullet+}$ (Calculated with the 6-31G* Basis Set)

	UHF	CASSCF[c]	UMP2
rhombus[d]	−155.759331	−155.83348	−156.26915
square[e]	+21.1	+20.5	+20.7

[a] For geometry see Figure 2. [b] R_{C-C} = 1.575 Å, R_{C-H} = 1.080 Å, ∠(HCH) = 115.9°, calculated with "rhombic" MO's. [c] For definition of active space, see text. [d] Total energies in au. [e] Energy relative to rhombus in kcal/mol.

a large distortion from planarity (see Figure 4). Vibrational analysis confirmed that the puckered rectangle is a saddle point for the interconversion of equivalent rhombic minima with one negative frequency of −260 cm^{-1}.

The results of single-point UMP2/6-311G** and QCISD(T)/6-31G* energy evaluations at all considered geometries (for the D_{2h} and D_2 stationary points corrected by UMP2/6-31G* ZPE) are shown in Table I. From this it follows that neither an improvement of the correlation method nor an augmentation of the basis set changes the picture significantly. Apart from the calculations mentioned above, we also reoptimized the D_{4h} symmetric square structure at the UMP2/6-31G* level.

As shown by Borden et al.[14] for the related case of the square cyclobutadiene radical cation, the choice of the symmetry-adapted representation of the degenerate HOMO may significantly influence the computed energies. Therefore we evaluated UMP2 and UHF energies for the (optimized) square assuming either rhomboid or rectangular symmetry of the MO's (for a more detailed discussion see refs 4, 14, and 15). We found an energy difference of 1 kcal/mol on the UHF level which was reduced to a negligible value of 0.1 kcal/mol after accounting for MP2 correlation energy. It therefore appears that $CB^{\bullet+}$ does not suffer from this problem in such a dramatic way as it was demonstrated in the case of cyclobutadiene radical cation[14] and that, in fact, this artifact can be neglected at the UMP2 and QCISD(T) levels of theory.

In order to ascertain that the single-determinant description which is at the base of our calculations of the P.E.S. of $CB^{\bullet+}$ is adequate, we performed single-point CASSCF calculations as defined in section II) on all stationary points of the UHF and UMP2 surfaces as well as for square $CB^{\bullet+}$. These showed that in all cases one leading configuration accounts for more than 94% of the MCSCF expansion and that no other single configuration contributes more than 0.5%. Consequently, CASSCF reoptimization of the UHF stationary points did not lead to any significant geometric changes, and the nature of the P.E.S. was preserved. As an example, Table II shows the relative UHF, CASSCF, and UMP2 energies of the UMP2 global minimum (rhombus) and the square, which was calculated with the "rhombic" MO's for consistency.

These problems being solved, we calculated vertical (I_v) and adiabatic ionization energies (I_a) of CB. Using (U)MP2 optimized geometries, I_v was found to be 10.81 eV at the QCISD(T) level. Due to the strong JT distortion in $CB^{\bullet+}$, I_v of CB cannot be determined straightforwardly from the photoelectron (PE) spectrum.[16] However, the present value is in excellent agreement with two different electron-impact ionization threshold determinations which gave I_v = 10.6 ± 0.1 eV.[17] More importantly, the relaxation energy of vertically formed $CB^{\bullet+}$ is calculated to be 27.4 kcal/mol at the QCISD(T) level, which puts I_a(CB) at 9.62 eV, i.e. about 0.3 eV below the onset of the first PE band of CB. The large amount of excess energy imparted on vertically formed $CB^{\bullet+}$ may explain why this cation was found to rearrange with great efficiency even if formed close to threshold.[18]

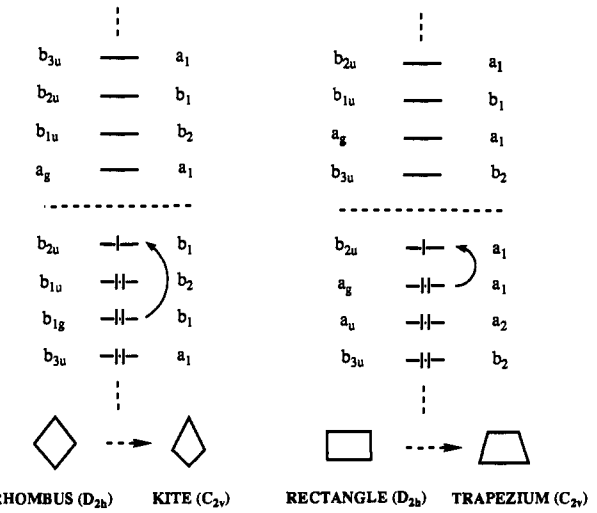

Figure 5. MO scheme for the D_{2h} and C_{2v} structures of $CB^{\bullet+}$ (arrows show the lowest lying excitations which could be held responsible for the SOJT).

In the hope of finding a single or a few low-lying configurations which could be held responsible for the proposed SOJT distortions (see Introduction), we performed limited CI calculations on the D_{2h} structures. It turned out, however, that the first excited configuration which could mix with the ground state upon lowering the symmetry toward C_{2v} lies 4 eV above the ground state for the rectangle and 6 eV above for the case of rhombus. According to a rule of thumb proposed by Pearson,[8b] excited configurations which lie more than 4 eV above the ground state generally do not mix strongly enough with the latter to induce SOJT distortions. The corresponding MO scheme with symmetry labels given both for the D_{2h} and C_{2v} structures is shown in Figure 5.

Therefore, the aim of further calculations was to find an answer to the questions why the relative stability of the C_{2v} and D_{2h} structures is reversed and why there are, in fact, no stable C_{2v} structures when a significant part of the correlation energy is accounted for. Thus, we performed CISD calculations based on the ROHF wave function, gradually enlarging the CI active space. It turned out that even when the six highest occupied MO's (including the two pairs of MO's degenerate in the square geometry) and the corresponding virtual orbitals are included into the CISD active space, the C_{2v} species remain more stable, although the energy difference between them is reduced by some 30–40%. It is only after all except the four 1s carbon core orbitals are included in the CISD active space that the D_{2h} structures become more stable.

In order to check if our theoretical predictions on the structure of $CB^{\bullet+}$ are in accord with experimental evidence,[2] ESR coupling constants were evaluated for a series of puckered rhomboidal geometries. Test calculations at the planar geometry were performed on the ROHF and CISD levels using 6-31G to 6-311G** basis sets. The active space for CISD included either the six highest occupied MO's and corresponding virtual orbitals ("small CI") or the whole set of MO excluding only the four 1s carbon ones. We found that the 6-31G basis set was adequate

(14) Borden, W. T.; Davidson, E. R.; Feller, D. *J. Am. Chem. Soc.* **1983**, *105*, 6775.
(15) Jungwirth, P.; Čársky, P.; Bally, T. *Chem. Phys. Lett.* **1992**, *195*, 371.
(16) (a) Bischof, P.; Haselbach, E.; Heilbronner, E. *Angew. Chem.* **1970**, *82*, 952. (b) Gleiter, P. *Top. Curr. Chem.* **1979**, *86*, 197.
(17) (a) Pottie, R. F.; Harrison, A. G.; Lossing, F. P. *J. Am. Chem. Soc.* **1961**, *83*, 3204. (b) Meisels, G. G.; Park, J. Y.; Giessner, B. G. *J. Am. Chem. Soc.* **1970**, *92*, 254. The ionization threshold of CB is expected to be slightly lower than I_v because $CB^{\bullet+}$ can also be formed nonvertically (albeit with lower efficiency) in electron impact experiments.
(18) Hughes, B. M.; Tiernan, T. O. *J. Chem. Phys.* **1969**, *51*, 4373 and references cited therein. For more details on the rearrangement and fragmentation of $CB^{\bullet+}$, see also the following paper in this series.

Table III. ESR Hyperfine Coupling Constants (in G) for the Four Nonequivalent Hydrogens of the Puckered Rhomboidal $CB^{\bullet+}$ as a Function of the Puckering Angle α (See Figure 4) Calculated on the ROHF and CISD Level and Compared with Iwasaki's Experimental and INDO Results[2]

α (deg)	method	$a(H_1)$	$a(H_2)$	$a(H_3)$	$a(H_4)$	$a(H_3)-a(H_4)$
180	ROHF/6-31G*	0.0	0.0	30.9	30.9	0.0
	ROHF/6-311G**	0.0	0.0	29.9	29.9	0.0
	small CISD[a]/6-31G*	-2.6	-2.6	34.7	34.7	0.0
	CISD/6-31G*	-4.9	-4.9	37.6	37.6	0.0
	CISD/6-31G	-6.8	-6.8	39.4	39.4	0.0
175	CISD/6-31G	-6.8	-6.9	45.1	33.9	11.2
170	CISD/6-31G	-6.7	-6.9	50.7	28.6	22.1
168	INDO[b]	-7.9	-11.9	50.5	25.5	25.0
	CISD/6-31G	-6.7	-6.9	53.5	26.1	27.4
165	CISD/6-31G	-6.6	-6.9	56.1	23.7	32.4
?	ESR experiment[b]	≈5	≈5	49 (44)[c]	14 (22)[c]	35 (22)[c]

[a] For definition see text. [b] Reference 2. Note that Iwasaki et al. define puckering via the C_1–C_2–C_3 and C_2–C_3–C_4 angle (109.3 and 68.9°, respectively), which works out to give $\alpha = 168°$ in our definition. [c] Values in parentheses are after annealing at 77 K and refreezing to 4 K (see ref 2).

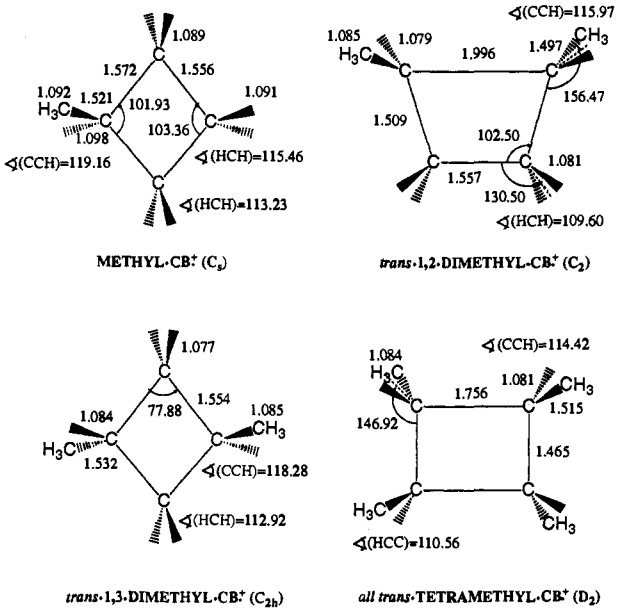

Figure 6. UHF/6-31G* optimized geometries of selected alkyl derivatives of $CB^{\bullet+}$ (The C–H bond lengths of the methyl groups were always within 0.001 Å of the indicated value, and the HCC angles were 110.4° ± 0.2 in all cases).

and that large CISD was necessary to achieve saturation with respect to the treatment of correlation effects, so the calculations on puckered structures were done at this level. Our results as well as those obtained from ESR experiments and semiempirical INDO calculations by Iwasaki et al.[2] are summarized in Table III.

V. Mono-, Di-, and Tetramethyl Derivatives of $CB^{\bullet+}$: Results

In order to investigate the influence of substituents on the Jahn–Teller P.E.S. of $CB^{\bullet+}$ and on the relative stability of the D_{2h} and C_{2v} structures, a series of methylated derivatives of $CB^{\bullet+}$ were studied. One of them, *all-trans*-tetramethyl-$CB^{\bullet+}$, is a "true" JT active species while the others, methyl-$CB^{\bullet+}$, *trans*-1,2-dimethyl-$CB^{\bullet+}$, and *trans*-1,3-dimethyl-$CB^{\bullet+}$, are subject to pseudo-JT effects, since the original electronic degeneracy is slightly lifted by the nonsymmetric influence of the substituents.

Four geometries of monomethyl-$CB^{\bullet+}$ corresponding to those of the parent cation described above were studied at the UMP2/6-31G*//UHF/6-31G* level. Since the molecule posseses low

Table IV. UHF/6-31G* and UMP2/6-31G*//UHF/6-31G* Energies of Selected Mono-, Di-, and Tetramethyl Derivatives of $CB^{\bullet+}$

compound	structure	UHF/6-31G*	UMP2/6-31G*
methyl-$CB^{\bullet+}$	kite[a,b]	-194.803424	-195.44609
	trapezoidal C_4 frame[c]	-13.4	3.7
	rectangular C_4 frame[c]	-5.5	2.0
trans-1,2-di-methyl-$CB^{\bullet+}$	trapezium[b]	-233.872210	-234.62171
	rectangular C_4 frame[c]	10.4	0.7
trans-1,3-di-methyl-$CB^{\bullet+}$	rhombus[b]	-233.845955	-234.62377
	kite-shaped C_4 frame	collapsed to the rhombus	
all-trans-tetra-methyl-$CB^{\bullet+}$	rectangle[b]	-311.939028	-312.97482
	trapezium[c]	-6.5	4.6
	kite[c]	22.7	16.0
	rhombus[c]	24.4	16.2

[a] Nearly rhombic geometry. [b] Total energies in au. [c] Energies relative to the most stable structure at the UMP2/6-31G* level (in kcal/mol).

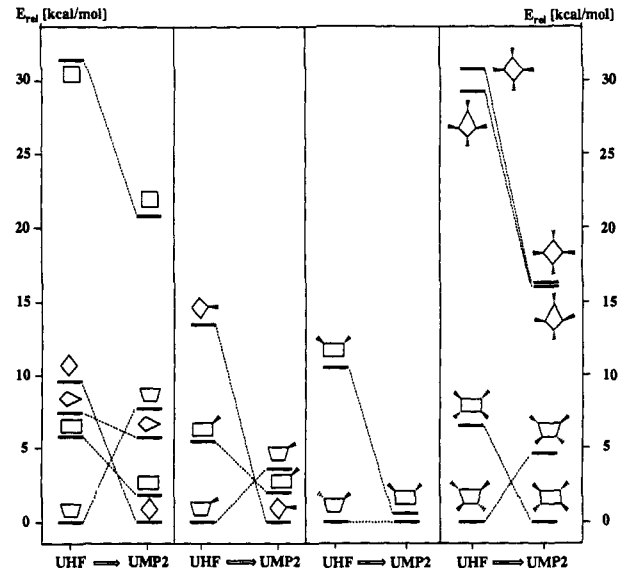

Figure 7. Schematic plot of the relative energies of cyclobutane radical cation and its alkylated derivatives.

(C_1 or C_s) symmetry, all geometries tend to collapse to the HF global minimum. Therefore, the carbon frame of the ring was constrained to remain planar and hold rhombic (D_{2h}), rectangular (D_{2h}), trapezoidal (C_{2v}), and kite shapes (C_2), respectively (Figure 6 and Table IV). Finally, an unconstrained UMP2 optimization was performed which led to a planar kite structure with only minor deviation from rhombic geometry. A similar level of theory was applied to the dimethyl derivatives of $CB^{\bullet+}$. However, only planar symmetric geometries, i.e. the rectangle and trapezium for *trans*-1,2-dimethyl-$CB^{\bullet+}$ and rhombus and kite for *trans*-1,3-dimethyl-$CB^{\bullet+}$, respectively, were studied in more detail (Figure 6 and Table IV). Unconstrained UHF/6-31G* optimization led to a planar trapezium in the former case while in the latter case planar rhombus was found to be the optimal structure (see Table IV).

Since tetramethyl-$CB^{\bullet+}$ possesses the same symmetry as the parent molecule, a similar strategy in exploring the P.E.S. was applied. D_{2h} and C_{2v} geometries were optimized at the UHF level, followed by UMP2 single-point energy evaluations. The stability toward puckering was then tested. The rectangle and the trapezium were found to be planar, but the rhombus and kite were puckered 32° and 31°, respectively. At the UMP2 level the rectangle is the most stable structure followed by the trapezium. The kite and the rhombus have nearly the same energy, being, however, 16 kcal/mol less stable than the rectangle, in contrast to the parent molecule and its monomethyl derivative.

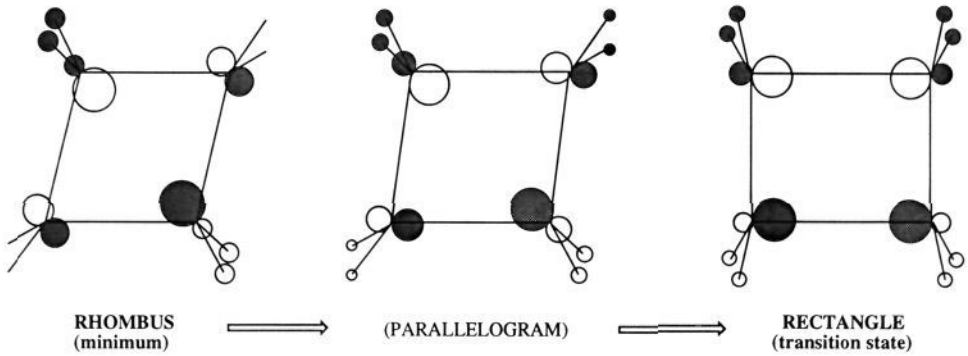

Figure 8. Change of the shape of the singly occupied HOMO during the rhombus → rectangle interconversion (MOPLOT[22] representation of ROHF/3-21G wave functions).

VI. Discussion and Conclusions

The main conclusion of the present study, summarized schematically in Figure 7, is that correlation plays a pivotal role in shaping the potential energy surface of $CB^{\bullet+}$ and its methylated derivatives. In particular, the stationary points of C_{2v} symmetry found by using various flavors of single-determinant SCF theory turn out to be spurious if correlation is taken into account.[19] This is already borne out by perturbation theory carried to second order with basis sets of moderate size, and neither a more complete account for correlation nor an augmentation of the basis set appears to affect this picture significantly (cf. Table I). Luckily, the UHF wave functions in all the studied regions of the $CB^{\bullet+}$ P.E.S. were found to be only slightly contaminated by higher spin states, such that the Møller–Plesset perturbation series is expected to converge reasonably well and MP2 results should be trustworthy.[20]

Limited-space CISD calculations demonstrated that the correlation effect responsible for the dramatic stabilization of the symmetric delocalized vs the long-bond trapezoid structures favored on the HF level is of dynamic nature: CI including the most important valence and the corresponding virtual MO's did not lead to a reversal of the HF picture. The same calculations showed also that the rectangle → trapezium and the rhombus → kite distortions found at the HF level cannot be attributed to a second-order Jahn–Teller effect because the excited configurations which could in principle induce this lie too high in energy to cause a distortion to lower symmetry. In view of the recently discussed case of propane radical cation,[21] we conclude that probably no special effects are operative in $CB^{\bullet+}$ but that single-determinant SCF theory simply overestimates the stability of long-bond structures in ionized saturated hydrocarbons.

That such long-bond structures do, however, exist is shown by the effect of methyl substitution. Already a single methyl group reduces the preference for the first-order JT structures by 40% while two vicinal methyl groups in a *trans* configuration suffice to revert the order and make the long-bond structure marginally more stable (cf. Figure 8). Interestingly, the symmetric structure is favored again in the tetramethyl derivative, which shows that steric effects also play an important role in shaping the P.E.S. of radical cations containing four-membered rings. Presumably, the "electronically favored" trapezium is put at a steric disadvantage because it has three C–C bonds of normal length vs two in the rectangle. Nevertheless we can conclude that electron-donating substituents may serve to stabilize long-bond structures to the extent where they become preferred over the more symmetric delocalized ones.

Returning to the region of the JT surface of parent $CB^{\bullet+}$ which encompasses the stationary points, we note that it is extremely flat, both with respect to the interconversion between the FOJT structures and with respect to ring puckering (cf. Table I and Figure 4, respectively). At the UMP2/6-31G* level the activation barrier for the pseudorotation on the JT "sombrero" P.E.S. (i.e. interconversion between equivalent rhombic structures via rectangular transition states) is merely 1.9 kcal/mol and the higher level calculations show that this barrier may drop below 1 kcal/mol if the basis set is saturated and correlation is recovered more completely. Figure 8 shows how the singly occupied MO smoothly changes during the rhombus → rectangle interconvertion which passes via a parallelogram. In view of the experimental finding of a static rhomboid structure at 4 K, we note that solvation will tend to stabilize the rhombus (which has its charge localized on two CH_2 groups) relative to the completely delocalized rectangle.

Since the ESR spectra unequivocally established a significantly nonplanar structure of $CB^{\bullet+}$ at 4 K, we devoted special attention to the question of puckering. As a matter of fact, our best calculations predict that the (observed) $^2B_2$ state, which actually represents the global minimum on the Jahn–Teller P.E.S., is planar, in contrast to the rectangular transition state which is strongly puckered (cf. Figure 3). However, the ≈10–15° deviation from planarity which is necessary to explain the observed hfc difference between axial and equatorial protons (cf. Table III) is accompanied by an energy increase of merely 0.05 kcal/mol which can easily be offset by the energy gained through better packing of the frozen freon solvent.

It is also interesting to note in this context that, immediately after ionization at 4 K, the above mentioned difference in ESR hyperfine coupling constants (hfc) is significantly larger (35 G) than that after annealing to 77 K (where averaging of all proton hfc's occurs) and subsequent refreezing (22 G). Perhaps in the absence of a strong driving force toward planarity, the rigid environment prevents incipient $CB^{\bullet+}$ from relaxing significantly from the puckered geometry of neutral CB (168°). At 77 K the rapid pseodorotation on the JT surface provides sufficient room for $CB^{\bullet+}$ to attain the optimal puckering angle (which according to our calculations should be 180° at the rhomboidal geometry) while subsquent refreezing results in the observed best compromise between optimized packing of the solvent and reduction of the solute's volume through puckering.

Finally we note that the minimum-energy structures of all methylated derivatives of $CB^{\bullet+}$ were found to be planar (although still very flexible, as shown by the frequencies of the puckering vibrations). However, we should point out that the derivatives were optimized at the UHF rather than the UMP2 level and that

(19) It is interesting to mention in this context that to the best of our knowledge first calculation on the P.E.S. of $CB^{\bullet+}$ on the MINDO/2 level correctly predicted the rhombus to be the global minimum.[16a] However, it is very likely that the authors restricted their search only to D_{2h} structures.

(20) See e.g.: Andrews, J. S.; Jayatilaka, D.; Bone, R. G. A.; Handy, N. C.; Amos, R. D. *Chem. Phys. Lett.* **1991**, *183*, 423 and references therein.

(21) Lunell, S.; Feller, D.; Davidson, E. R. *Theor. Chim. Acta* **1990**, *77*, 111.

(22) Haselbach, E.; Schmelzer, A. *Helv. Chim. Acta* **1971**, *54*, 1299. Version for DOS-PC's (adapted to display split valence ab initio MO's by P. Jungwirth) is available from T. Bally upon request.

the possible subtle effects of correlation on the puckering P.E.S. have thus not been accounted for.

Acknowledgment. This work is part of project No. 20-34071.92 of the Swiss National Science Foundation. We are very indebted to IBM Switzerland for the loan of an RS/6000 workstation without which this project would have been impossible to carry out. P.J. would like to thank the Office for Social Services of the University of Fribourg for a stipend and Prof. Edwin Haselbach for his hospitality and for exciting discussions.